6.2 ATOMISTIC STUDIES OF PROPERTIES OF HELIUM IN BCC IRON USING THE NEW He–Fe POTENTIAL

—David M. Stewart, Stanislav Golubov (Oak Ridge National Laboratory and the University of Tennessee), Yuri Ostesky, Roger E. Stoller, Tatiana Seletskaia, and Paul Kamenski (Oak Ridge National Laboratory)

OBJECTIVE

The objective of this work is to use molecular dynamics techniques to increase understanding of the behavior of transmutation-produced helium in reduced-activation ferritic/martensitic steels that are candidate materials for fusion reactors. As there is no suitable iron-carbon-helium interatomic potential, simulations are performed using helium in pure iron.

SUMMARY

We have performed atomistic simulations of helium bubble nucleation and behavior in iron using a new 3-body Fe–He inter-atomic potential combined with the Ackland iron potential. Updated results from ongoing large simulations examining the nucleation of helium defects are presented. When an Fe interstitial encounters a helium bubble, it can recombine with one of the vacancies in the bubble, leading to a bubble with a higher He/V ratio and hence higher pressure. We investigate how far this process can go before the bubble will not accept any more SIAs.

PROGRESS AND STATUS

Introduction

Helium produced in neutron irradiated iron affects the mechanical properties. The growth, migration and coalescence behavior of helium bubbles is very sensitive to the assumed properties of individual He interstitials and helium-vacancy clusters [1]. A new He–Fe inter-atomic potential has been developed at ORNL, based on extensive fitting to first-principles calculations of point defects and clusters [2–4]. This potential has been used to investigate the properties of helium, helium-vacancy clusters and helium bubbles in MD and MS simulations.

Helium diffuses very fast in the matrix, but is easily trapped in vacancies [5]. It is possible for a self-interstitial to recombine with the vacancy, knocking the helium back into an interstitial position. Previous calculations [6] showed that recombination is possible not only for a single substitutional He, but even when the vacancy contains multiple Helium atoms. The reverse process (i.e. Frenkel pair formation) can happen—an iron atom is pushed out of its lattice site, creating a He–V cluster and an SIA. As more helium joins the cluster, more Frenkel pairs are formed, creating larger defects. These mechanisms are investigated together in larger simulations [6] that examine the nucleation of He defects. Some of these simulations are ongoing, with the latest results presented here.

The He–V defects nucleated in this manner are nascent bubbles. Helium bubbles are more stable than voids and continue to grow as more helium and vacancies diffuse to the bubble. Helium bubbles of sizes 1–6 nm were studied in [6]. In order to estimate the amount of helium present from an observed bubble size distribution, it is necessary to understand the relationships between bubble size, pressure and helium content. Extensive atomistic simulations of such bubbles were compared to show effect of temperature, interatomic potentials used and helium concentration. Here we extend that by investigating the interaction of bubbles with a surplus of self-interstitial atoms. We also determine the surface energy of a bubble made up of specific crystallographic facets.

Simulation Method

For the MD simulations reported here, the general procedure followed is: Generate perfect BCC lattice. Introduce the defect(s) to be studied. Relax at constant volume using a mixture of conjugate gradient and simulated annealing, and save the atom positions in units of the lattice constant. Start the simulation.

The MD simulations used NVE (constant **n**umber of atoms, constant **v**olume and constant **e**nergy) dynamics. The lattice constant and initial velocities were chosen to give close to zero pressure and the desired initial temperature. The boundary conditions are periodic in *X*, *Y* and *Z*, which are ⟨100⟩ directions. The velocity Verlet algorithm with a timestep of 0.3fs is used. As volume and temperature correction are not used, when processes that release energy are simulated the temperature and pressure both rise during the simulation.

The potentials used are the ORNL He–Fe potential [2–4], the Ackland Fe–Fe potential [7] and the Aziz He–He potential [8]

Coalescence

Previous He coalescence simulations [6,9,10] were run at four different sizes/concentrations. The smaller ones are 125 helium atoms in a 31×31×31 BCC iron matrix (60,000 iron atoms) and 125 helium atoms in a 40×40×40 BCC iron matrix (128,000 iron atoms). These give concentrations of 2089 and 976 appm He respectively. In addition, much larger simulations are ongoing at two concentrations: 1000 and 500 helium atoms in a 80×80×80 BCC iron matrix (1,024,000 iron atoms). These give concentrations of 976 and 488 appm He respectively. All of these are simulated at 600 K and 1000 K. For all these simulations, the concentration of vacancies created is plotted as a function of time. The latest results are shown in Figure 1.

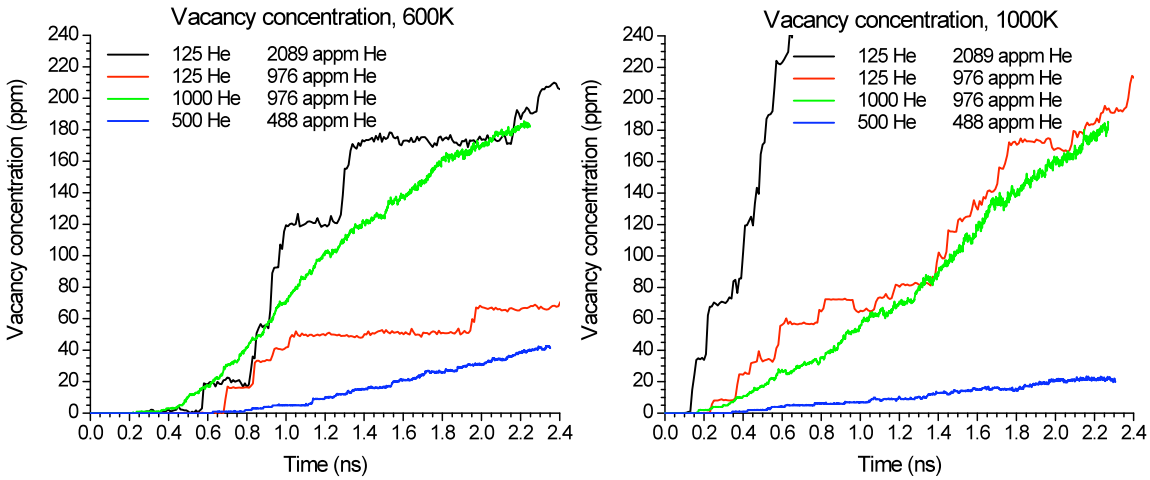

Figure 1. Coalescence for different concentrations at (a) 600 K and (b) 1000 K.

Interaction of bubble with SIAs

Self-interstitial atoms can recombine with some of the vacancies that make up a helium bubble, increasing the He/V ratio. This can lead to over-pressurized bubbles. There must be a limit to this; eventually the bubble will have to stop accepting SIAs (or invoke some other process such as ejecting helium, which seems unlikely).

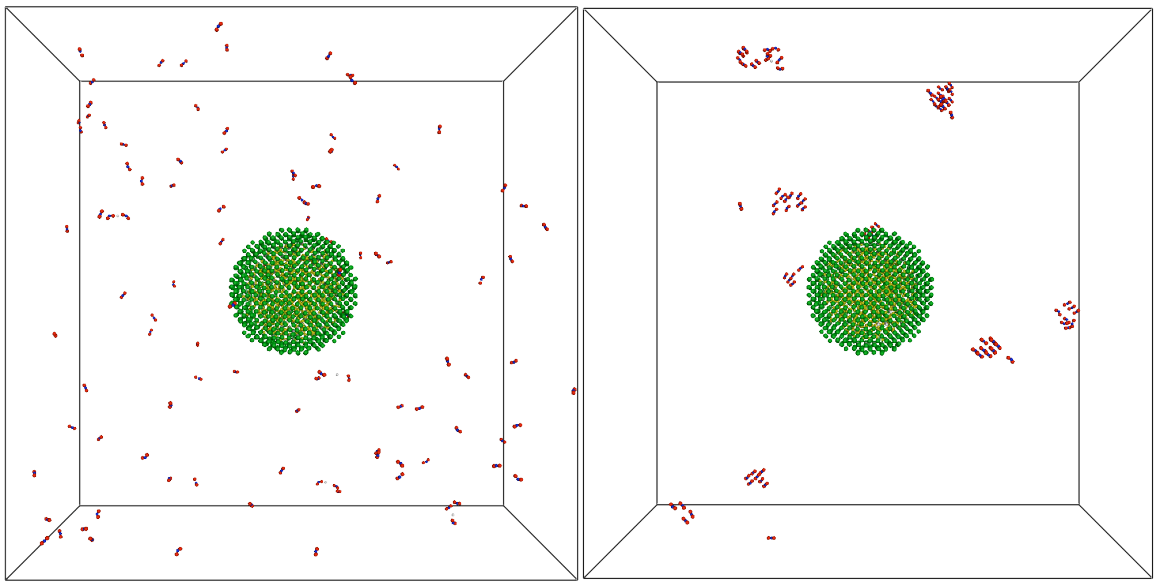

Figure 2. a) Initial condition. b) After 1ns

In order to investigate the recombination of SIAs with a large bubble, we simulated 100 SIAs near a 4nm helium bubble. The initial configuration is shown in Figure 2a. The bubble was in the center of the 60×60×60 periodic cell, and the SIAs were placed randomly in the lattice at least 4 lattice parameters from the bubble. Figure 2b shows the situation after 1 nanosecond of simulation time. The SIAs mostly clustered with each other instead of recombining with the vacancies in the bubble.

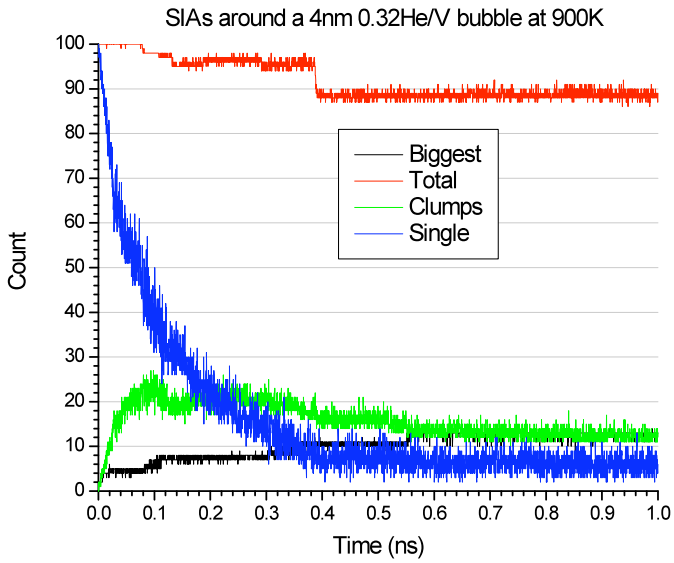

Figure 3. Recombination and clustering of SIAs around a 4 nm helium bubble. Black line: Size of largest cluster. Red: Total SIAs. Green: Clusters with 2 or more SIAs. Blue: Single SIAs.

Figure 3 shows the number of SIAs over time. In the nanosecond, 11 SIAs recombined with the bubble, 4 remained free and 85 formed 13 clusters. The biggest cluster contained 13 interstitials. SIA clusters larger that about 2 or 3 SIAs are only mobile in one dimension, which greatly reduces their chance of finding their way to the bubble. Larger SIA clusters have very little mobility at all. Eleven SIAs recombining with a bubble of 2,741 vacancies did not cause any substantial change in the bubble. Due to the clustering, it is unlikely that running the simulations longer would significantly increase the number of SIAs that recombine.

As small SIA clusters are observed to be mobile only in one dimension, a simulation that uses SIA clusters can arrange them so that they will move on a line that crosses the bubble. This allows us to set up another simulation that is better suited to testing the limit to how many SIAs the bubble will recombine with.

A 1 nm bubble was placed at the center of a 30×30×30 box. An SIA cluster, consisting of seven SIAs, was placed 17 lattice parameters away in each of the eight ‹111› directions. Each cluster was oriented towards the bubble, so its only possible motion is towards the bubble or directly away from it. The bubble had 59 vacancies and different amounts of helium in each run. The clusters had a total of 56 SIAs. Figure 4 shows the starting and ending configuration for an equilibrium (23 He at 900 K) bubble.

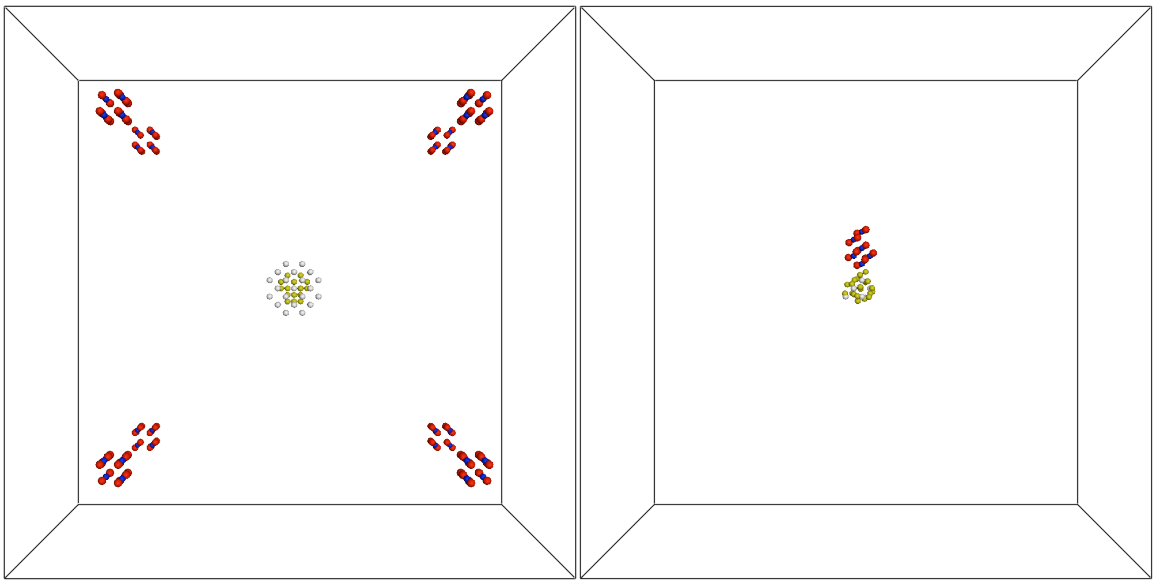

Figure 4. a) Initial condition. 23 He, 59 V b) After 3ns

Simulations were run at 900 K for different amounts of helium in the bubble, from 5 to 95 atoms. Each SIA cluster was seen to do one of two things. It could move in and recombine with the bubble, or it could move away and merge with other clusters.

The final number of vacancies as a function of the number of helium atoms is plotted in figure 6a. For 5 He atoms, all 8 clusters recombined, leaving three vacancies.

For 10–30 He atoms, some of the clusters recombined with the bubble and the rest merged together. The merged cluster eventually collided with the bubble and partially recombined, leaving a bubble with a smaller cluster of SIAs attached. The final position for 15, 23 and 30 He atoms can be seen in figures 5a, 4b and 5b respectively.

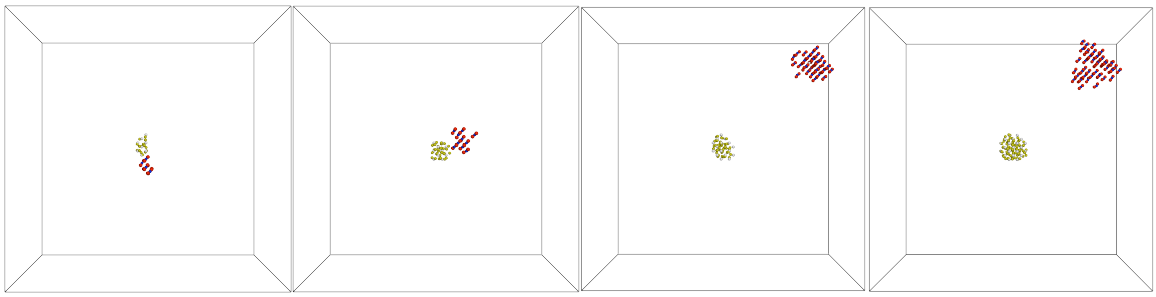

15He 3ns | 30He 3ns | 45He 3ns | 85He 1ns

Figure 5. Final positions for different He/V ratios. All bubbles have 59 Vacancies

For 35 and more He atoms, again some of the clusters recombined with the bubble and the others merged. But this time the merged cluster did not encounter the bubble within the simulation time (1–3 ns). The final position for 45 and 85 He atoms can be seen in figures 5c and 5d respectively. Note that in figure 6a, the final number of vacancies is always 59 minus a multiple of 7, as each cluster has 7 SIAs.

The final He/V ratios as a function of the number of helium atoms is plotted in figure 6b. They have a wide range: from 1.1 to 2.3. The average is 1.66.

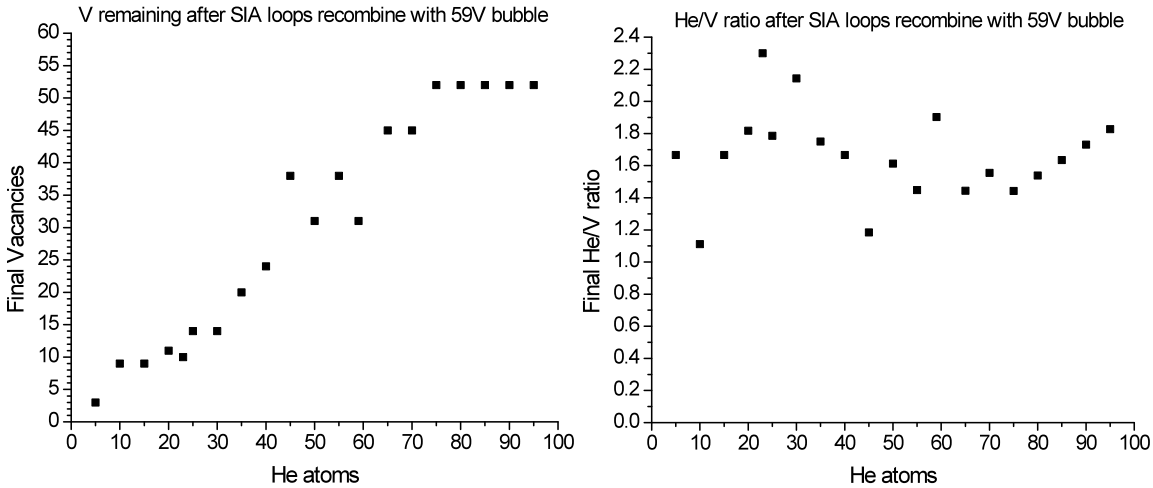

Figure 6. Final number of vacancies/Final He/V ratio in the bubble for different numbers of helium atoms. All bubbles had 59 vacancies initially.

Surface energy of voids

As different crystallographic facets have different surface energies, the shape of a void may influence the pressure of gas it can hold. The surface energy of voids of different shapes is calculated. Energy is calculated by molecular static relaxations. Surface area is calculated from the number of vacancies (i.e. the volume) using the appropriate geometric formula for the shape. A plot of energy vs. surface area is shown in figure 7.

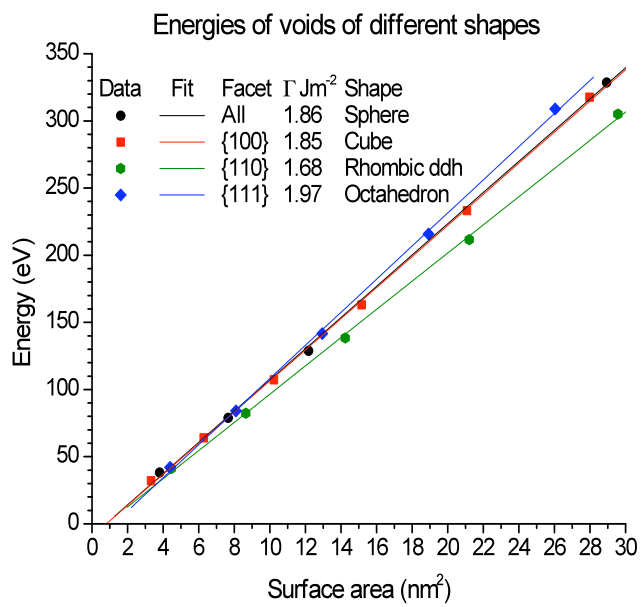

Figure 7. Energy vs surface area of different shaped voids

The four different shapes considered are shown in figure 8. The sphere has a minimum total surface area for a given volume. The cube, rhombic dodecahedron and octahedron consist of only {100}, {110} and {111} surfaces respectively. The results show that the {110} surface has the lowest energy, followed by the {100} surface and lastly by the {111} surface. As one would expect, the result from the sphere is in between as the sphere contains a mixture of different surfaces.

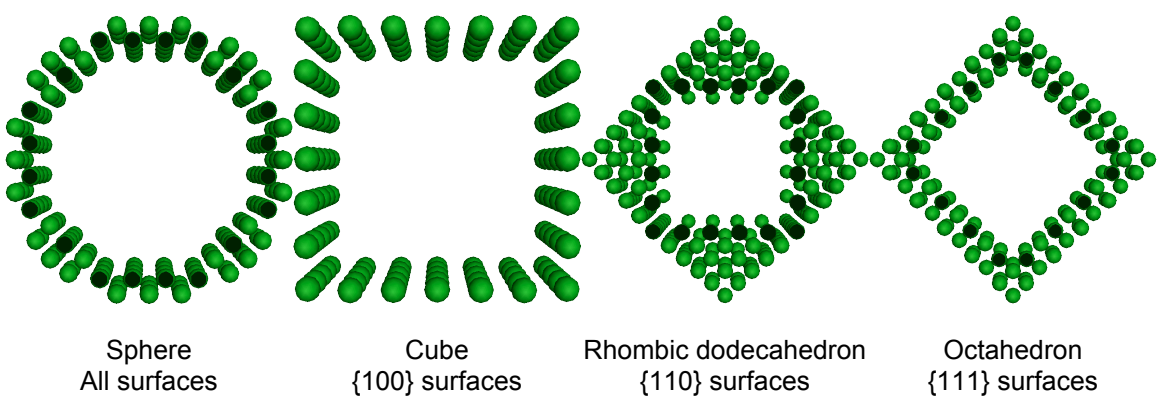

Figure 8. Cross-sections of the four different shapes of void investigated.

References

[1] S.I. Golubov, R.E. Stoller, S.J. Zinkle, and A.M. Ovcharenko, Kinetics of coarsening of helium bubbles during implantation and post-implantation annealing, Journal of Nuclear Materials 361 (2007), pp. 149–159.

[2] T. Seletskaia, Y.N. Osetsky, R.E. Stoller, and G.M. Stocks, Magnetic Interactions Influence the Properties of Helium Defects in Iron, Physical Review Letters 94 (2005), pp. 046403.

[3] T. Seletskaia, Y.N. Osetsky, R.E. Stoller, and G.M. Stocks, Calculation of helium defect clustering properties in iron using a multi-scale approach, Journal of Nuclear Materials 351 (2006), pp. 109–118.

[4] T. Seletskaia, Y.N. Osetsky, R.E. Stoller, and G.M. Stocks, Development of a Fe He interatomic potential based on electronic structure calculations, Journal of Nuclear Materials 367 (2007), pp. 355–360.

[5] H. Trinkaus and B. Singh, Helium accumulation in metals during irradiation–where do we stand? Journal of Nuclear Materials 323 (2003), pp. 229–242.

[6] D.M. Stewart, July 2010 semiannual report.

[7] G.J. Ackland, D.J. Bacon, A.F. Calder, and T. Harry, Computer simulation of point defect properties in dilute Fe-Cu alloy using a many-body interatomic potential, Philosophical Magazine A-Physics of Condensed Matter Structure Defects and Mechanical Properties 75 (1997), pp. 713–732.

[8] R. Aziz, A. Janzen, and M. Moldover, *Ab Initio* Calculations for Helium: A Standard for Transport Property Measurements, Phys. Rev. Lett. 74 (1995), pp. 1586–1589.

[9] David M. Stewart, Yuri N. Osetsky and Roger E. Stoller, Atomistic studies of formation and diffusion of helium clusters and bubbles in BCC iron, In Press, Journal of Nuclear Materials

[10] David M. Stewart, Yuri N. Osetsky, Roger E. Stoller, Stanislav I. Golubov, Tatiana Seletskaia and Paul J. Kamenski, Atomistic studies of helium defect properties in bcc iron: comparison of He–Fe potentials, Philosophical Magazine, Volume 90, Issue 7 & 8 (March 2010) pp. 935 – 944